LABORATORY SIMULATION OF SHEAR BAND DEVELOPMENT IN A GROWTH NORMAL FAULT

Sheng-Shin Chu [1], Ming-Lang Lin [2], Wen-Chao Huang [3], Huan-Chi Liu [4], and Pei-Chen Chan [5]

ABSTRACT

Studies on active faults in the metropolitan Taipei area have indicated that the Shanchiao fault at the western rim of the Taipei Basin is a highly active normal fault. Fault slip can cause the deformation of shallow soil layers and lead to the destruction of residential building foundations, utility lines, and other infrastructure near the influenced area. The Shanchiao fault is considered a growth normal fault based on geological drilling and dating information. Therefore, a geological structure similar to a growth normal fault was constructed to simulate slip-induced ground deformation after an additional layer of sedimentation formed above the deformed normal fault. We employed a sand box with non-cohesive sands under normal gravity conditions to investigate the shear band propagation and surface deformation of a growth normal fault. In the presence of a sandy sedimentation layer on top of the deformed sandy soil layer caused by a normal fault, a shear band developed along the previous shear band and propagated upward to the sandy surface at a much faster speed compared to the case without a sedimentation layer (*i.e.*, normal fault only). An offset ratio of 1% ~ 1.5% (defined as the fault tip offset displacement over the soil layer thickness) for this particular growth fault simulation is required to develop a shear band toward the ground surface. The test results indicated that the shear band of a growth normal fault with sandy material could propagate to the ground surface only under a smaller offset displacement from the fault tip, although the depositional thickness of the upper layer might be very thick. Therefore, a seismic design integrated with the knowledge of near-ground deformation characteristics for this type of fault must be emphasized in current building codes, particularly for critical facilities such as a nuclear power plant.

Key words: Shanchiao fault, growth normal fault, sand box test, shear band, offset ratio.

1. INTRODUCTION

The Taipei metropolitan area (including Taipei City and New Taipei City that are within Taipei basin area) is located at the northwestern edge of the Pleistocene orogens in Taiwan. During and after the orogenic period, several types of fault-related structures were formed in this area. The investigation results of disastrous earthquakes indicate that when the fault fractured, most buildings near the fault traces suffered severe damage (Kelson *et al*. 2001; Konagai 2005; Bray and Kelson 2006). Consequently, the damage to roads, highways, and utility lines caused further loss of life and property. The Taipei metropolitan area is the major political and economic center in Taiwan; therefore, the presence of an active fault and its activity is a major concern of residents in this area and is also a research focus for academic researchers. (Wang 2008; Cheng *et al*. 2010).

Manuscript received December 21, 2012; revised April 21, 2013; accepted April 22, 2013.

[1] Ph.D. candidate, Department of Civil Engineering, National Taiwan University.

[2] Professor, Department of Civil Engineering, National Taiwan University.

[3] Assistant Professor (corresponding author), Department of Civil Engineering, National Central University (e-mail: wenchaoh@ncu.edu.tw).

[4] Adjunct Assistant Professor, Education Department of Earth and Life Science, Taipei Municipal University of Education.

[5] Ph.D. student, Department of Civil Engineering, National Taiwan University.

After the Pleistocene period, northern Taiwan was subject to the clockwise turning and westward extension effect of the Okinawa trough, and east-west horizontal stress replaced the original compression stress to become the main tectonic stress influencing crust formation in northern Taiwan. GPS survey data showed that the crust of the Taipei Basin and the adjacent area is stretching in the northwest-west to southeast-east direction (Yu *et al*. 1999). The thrust faults formed by compression stress during the orogenic period have become inactive and are not likely to become active again in the current geologic period (Lin 2005). However, the Shanchiao fault might still be a normal fault actively under the aforementioned tensile stress in the Taipei Metropolitan Area (*i.e.*, Taipei basin area). (Lin 2005). Furthermore, the Shanchiao fault was also found to be a growth normal fault (Huang *et al*. 2007; Chen *et al*. 2010), the deformation characteristics of a growth normal fault hence become the major focus in this study due to its potential activity.

2. GEOLOGICAL BACKGROUND OF THE SHANCHIAO FAULT

The Shanchiao fault is located at the west side of the Taipei basin in northern Taiwan and is a normal fault with a northwest strike and an eastward dip direction. Previous studies have indicated that the fault trace is along Guandu, Wugu, and Taishan to Shulin; however, the results of an evaluation by the Central Geological Survey of the Ministry of Economic Affairs in Taiwan showed that the Shanchiao fault trace also passes through the Datun volcanos and extends to the Jinshan area in the northeast

direction. The fault length is at least twice that of the previously recognized length (Central Geological Survey 2010). A geological survey commissioned by the Taiwan Power Company also indicated that this normal fault extends at least 40 km offshore (Fig. 1).

Although no seismic activity of the Shanchiao fault has been recorded, the apparent morphological scarp (as shown in Fig. 1) and 700 m depth of bedrock (1.7 m slip per one thousand years) located at the west side of the Taipei basin indicates that activity in the Shanchiao fault has played a critical role in the formation and evolution of the Taipei Basin. The eastward tensile stress mechanism in northern Taiwan could be a primary reason for the Shanchiao fault to become active again (Lee and Wang 1988; Lu *et al*. 1995; Teng 1996). Because the Shanchiao fault is covered by quaternary sediment (mostly lacustrine deposits) within the Taipei Basin, it is difficult to prove the existence of the fault. However, the Central Geological Survey and numerous engineering consultant companies have conducted drilling and seismic surveys for major construction projects that pass through the Shanchiao fault, such as the Xinzhuang line and airport line of Taipei's subway system. Surveying and drilling results have also contributed to a further understanding of the possible location of the fault, the depth of tertiary basal bedrock, and the top layer of quaternary sediment in the Taipei basin (Ever Transit International Co. Ltd. 1999; R.E.S. Inc. 1999).

The site investigation and drilling conducted by the Central Geological Survey since 1999 have completed the geological profiles of the Zhongyi, Guandu, Chengtsiliao, Wugu, and Shulin areas. Among these profiles, the SCF-5 and SCF-6 profiles corresponding to the Chengtsiliao and Wugu areas have shown that the tertiary basement was encountered in both profiles, but the depth of tertiary basement in SCF-6 is deeper than that of SCF-5 by approximately 100 m. The difference in basement depth of these two profiles could be evidence of the presence of the Shanchiao fault. Similarly, the SCF-15 and SCF-16 profiles (Figs. 2 and 3) showed basal depths of 52 m and 136.52 m with a significant depth difference of 84 m between these two profiles. Therefore, the trace of the Shanchiao fault is estimated to be located between these two drilling locations (Liu *et al*. 2000).

Drilling information indicates that the basal depth of the Shanchiao fault varies from 100 to 700 m (Lin 2005). Assuming that the ground surface elevation is 0 m, the sedimentary layer thickness of the Shanchiao fault may be somewhere between 100 and 700 m. A thick sedimentary layer (such as 700 m thickness) must have been deposited several times before and after the fault rupture, gradually increasing the sedimentary thickness. Because the sedimentary layer may not be formed under a single depositary event, it is necessary to explore the deformation effects of multiple sedimentary events with an underlying normal fault.

Following a single rupture event of a normal fault, the sedimentary layer typically forms from both the footing and hanging wall sides of the normal fault. Because the sedimentary layers in both sides were thick enough to become a single sedimentary layer, the sedimentary layer with the normal fault underneath is thus considered the growth normal fault. Several rupture events and sediment layers above the normal fault are also possible. From previous studies, the Shanchiao fault is also a growth normal fault based on drilling and dating information (Huang *et al*. 2007; Chen *et al*. 2010).

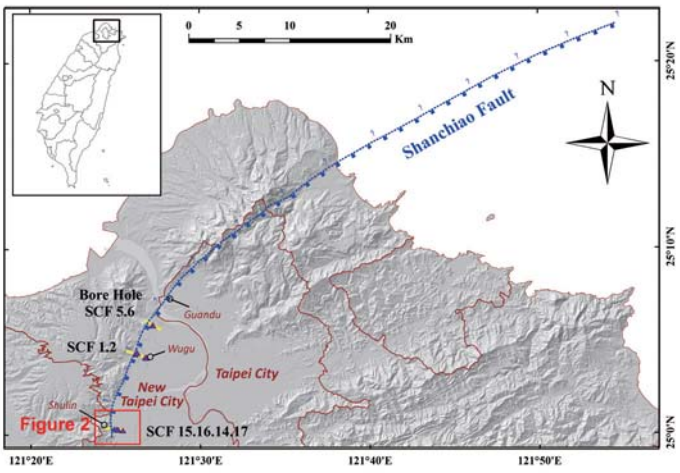

Fig. 1 Trace of Shanchiao Fault

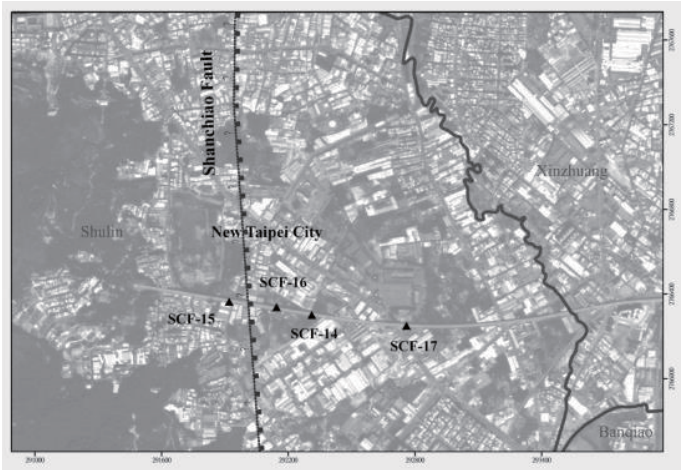

Fig. 2 Location of geological profiles SCF-15 and SCF-16

Recent approaches to studying the rupture of growth normal faults and the induced shear band propagation in the sedimentary layers have primarily focused on site investigation (Gawthorpe *et al*. 1997; Gawthorpe and Hardy 2002; Castelltort *et al*. 2004; Nicol *et al*. 2005; Taylor *et al*. 2008; Pochat *et al*. 2009), laboratory testing of normal faults (Hus *et al*. 2005; Lee and Hamada 2005; Patton 2005), and numerical simulations (Saltzer 1992; Seyferth and Henk 2006; Egholm *et al*. 2007; Nollet *et al*. 2012). In this study, laboratory testing is the primary research approach for understanding shear band propagation in growth normal faults.

3. METHODOLOGY OF GROWTH NORMAL FAULT SIMULATION

In this research, a small-scale physical model was used to explore the deformation behavior of the overlain layer caused by the offset of a growth normal fault. The sandbox experiment was scaled down to 1/300 of the Shulin (close to SCF-15 and SCF-16) cross section. A constant thickness of soil layer with dry sand at a constant fault dip angle was employed as the initial experiment state. After simulating a single event of a normal fault rupture by introducing a given offset displacement, another soil layer was

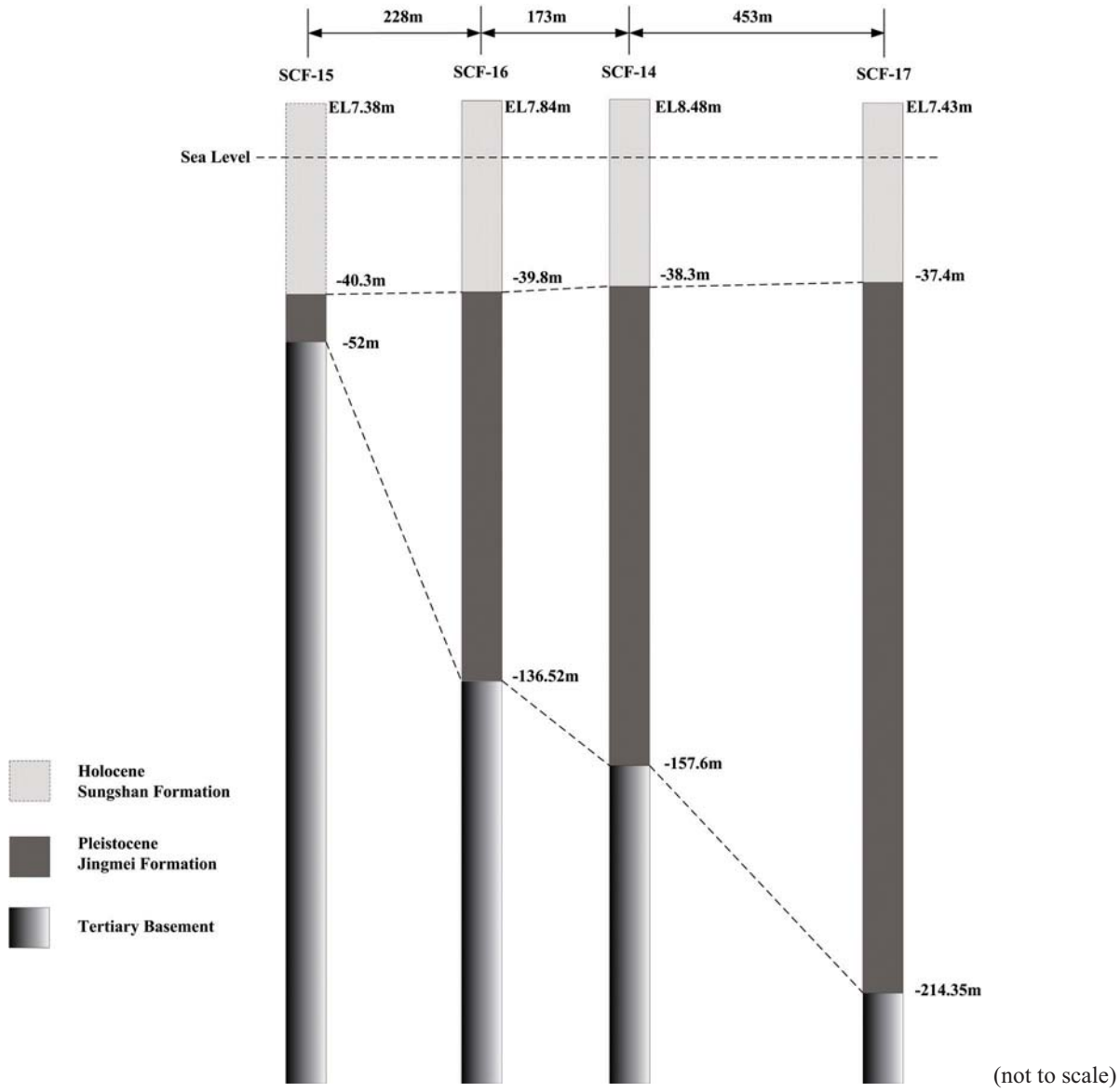

Fig. 3 Geological cross sections of profiles SCF-15 and SCF-16

then spread above the deformed ground surface. This situation was used as the basic model configuration before triggering any further offset. We expected that triggering the second offset displacement for the growth fault would cause the soil particles to form a failure plane that can develop to the ground surface. The offset displacement is the primary factor influencing shear band propagation and ground surface deformation width; therefore, we observed these two occurrences as the offset was increased to investigate the deformation mechanisms and the corresponding influenced zones.

3.1 Experimental Setup and Configurations

The sandbox dimensions are 100 cm in length, 20 cm in width, and 60 cm in height (Fig. 4). The bottom plate consists of a left and right panel. The left panel is a fixed part attached to the bottom of the sandbox. The right panel is a moving part controlled by the stepper motor to simulate fault ruptures of normal and thrust faults. The dip angle of the faults can be changed from 15 to 90 degrees at a 5-degree interval using an angle adjuster at the bottom of the basal driven system. The separation point of the right and left panel is defined by a gap in the bottom plate (similar to the location of the fault tip in bedrock). The testing material used in this experiment was Vietnamese quartz sand due to its high uniformity. The coefficients of uniformity and curvature are 2.08 and 0.9, respectively. To ensure a more uniform particle size distribution, the sands were also sieved between sieves no. 40 to no. 140. In addition, the specific gravity was 2.65 and the dry unit weight was 15.7 kN/m^3 under a relative density of 55% and a porosity of 0.68. The selection of the above relative density is to recreate a medium dense state for the testing material.

The experiment was conducted with the right panel moving downward along a plane with a 60-degree dip angle to simulate the effect of normal faulting, because a dip angle of 60 degrees can always represent a typical dip angle of normal fault (such as the Shanchiao fault). A 10-million-pixel camera mounted at a given distance from the sandbox sidewall took semi-continuous images during the test, including images of the development of

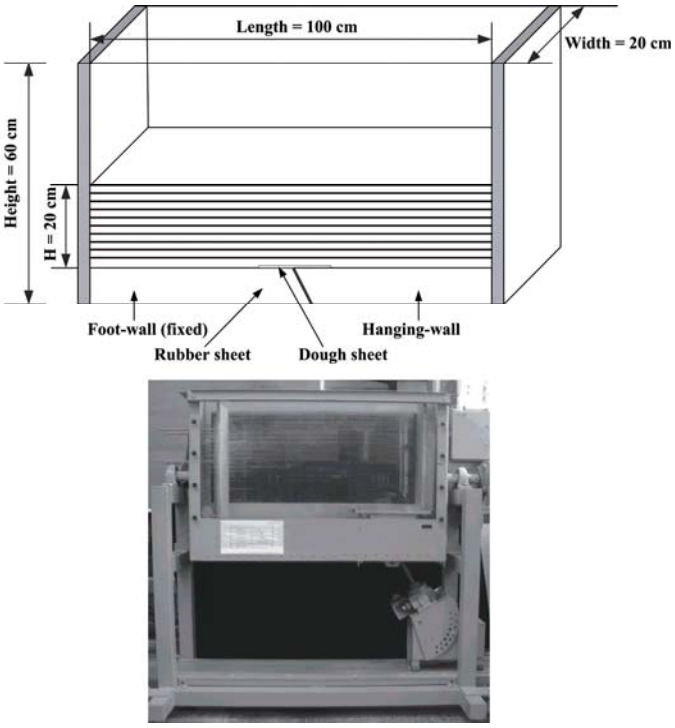

Fig. 4 Illustration and photo of sandbox

the failure plane in the sand layers. The oven-dried quartz sands were spread uniformly across the sand box layer by layer and several thin layers of quartz sands were pigmented and spread between sand layers 2 cm in thickness to clearly observe the shear band development. The purpose to employ oven-dried sands is to avoid any unnecessary cohesion of the sands and pigmented sands. The advantage of using colored quartz sands is that observations of colored sands at a given depth that are sheared (or any layer dislocation) indicate that the failure plane has propagated upward to that specific depth (Fig. 5).

3.2 Experimental Schemes

The sand box tests in this study were divided into three types. The first type (Type 1) involved creating a normal fault by triggering a one-time offset of 6 cm. The second type (Type 2) also involved creating a normal fault, but the offset from the fault tip was triggered with 3 cm offsets twice within 24 hours. The resultant offset was also 6 cm. The main purpose of conducting tests of Types 1 and 2 was to compare the shear band propagation caused by a delayed fault tip offset. The particle arrangements and the stress distribution could be re-organized after certain duration.

The third type of test (Type 3) involved creating a normal fault by triggering a 5 cm offset from the fault tip, and then allowing a layer of dry sand to fall freely from a given height of 30 cm to form a 1 cm-thick sand layer (1 cm thickness was measured from the ground surface of the footwall of the normal fault). After spreading the second layer on the deformed sand surface, another 1 cm offset was triggered from the fault tip to create another normal fault offset displacement to evaluate the shear band propagation and the influenced width measured from the sand surface in a growth normal fault. Semi-continuous photographs of all the above tests were taken and analyzed to understand the

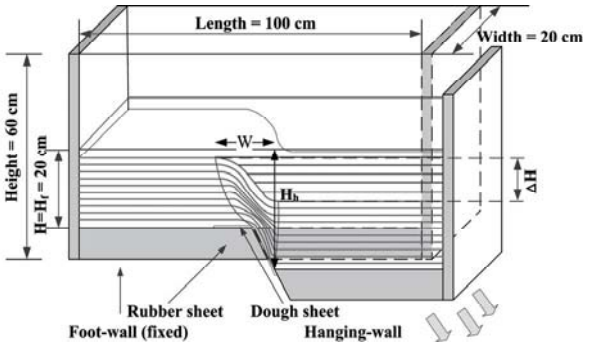

Fig. 5 Dislocation of pigmented sand layers after introducing an offset

stepwise deformation of the sand layers when an offset from the fault tip was introduced. These three tests were performed three times to prevent any deviations in the test results.

4. DISCUSSION OF TEST RESULTS

The pigmented sand layers were spread between sand layers 2 cm in thickness. Once the particle arrangement was changed by the offset of the fault tip, a shear band was clearly observed. The focuses of observation after tests were performed are the normalized width of the influenced zone (W/H, width, W, is normalized to the total thickness of the sand layer, H.) and how the shear band was formed in different types of tests. The width of the influenced zone (W) is the horizontal length between the vertical projections from the fault tip at the footwall sand surface to the tangent line of the footwall sand surface. The offset distance is termed as ΔH, and an offset ratio can be defined as $\Delta H/H$, which is a normalized offset distance according to the sand layer thickness. Because the total thickness of the sand layer, H, is different in footwall and hanging wall of the growth fault, the footwall sand layer thickness is defined as H_f and the hanging wall sand layer thickness is defined as H_h. The definitions of these quantities are also illustrated in Fig. 5.

The result discussions for each type of sandbox test are as follows:

Type 1: 6 cm offset at the fault tip

When the offset was introduced, the shear band initiated from the fault tip as expected. Increased downward vertical displacement of the hanging wall revealed upward shear band propagation toward the sand surface. The displacement photographs in Fig. 6 were taken under different offset distances. The influenced width (W) at the sand surface was measured to be approximately 30% ~ 50% of the sand layer thickness (H). When the offset ratio ($\Delta H/H$) reached 4.2% to 4.8%, the shear band developed to the sand surface.

Type 2: Two instances of 3 m offsets within 24 hour duration

The 6 cm offset distance was completed within 24 hours by introducing the 3 cm offset twice. The deformation photos were also taken under different displacement stages (Fig. 7). Because the 6 cm offset distance was introduced twice in this type of test,

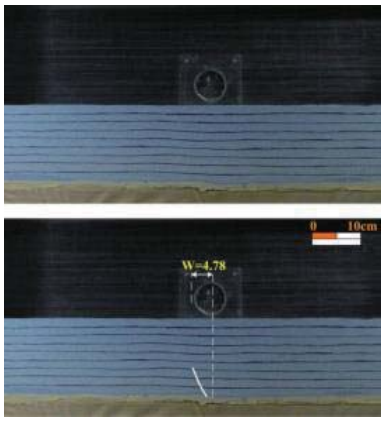

Step 1 –initiation of offset

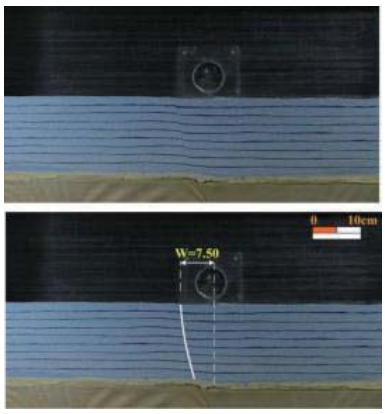

Step 2 –middle of test

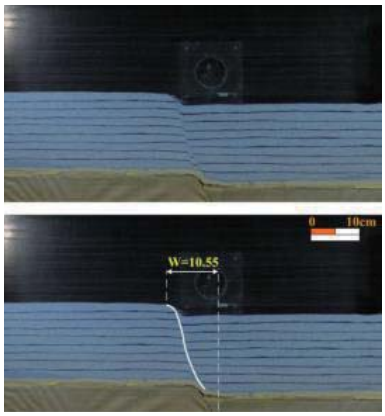

Step 3 –3 cm offset

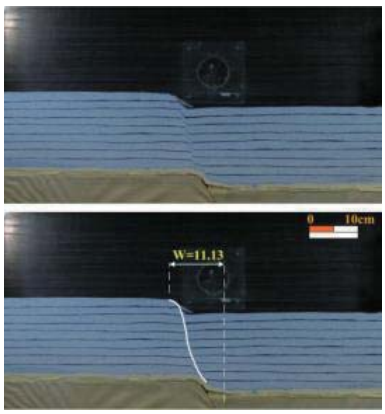

Step 4 –additional 0.7 cm offset

Fig. 6 Type 1 (6 cm offset from fault tip) shear band propagation photos

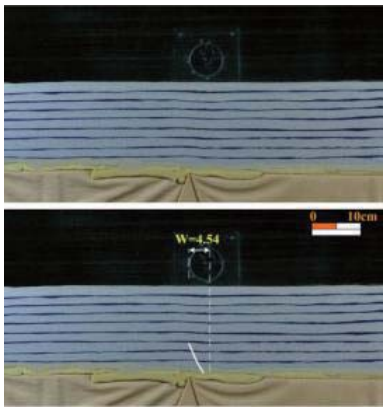

Step 1 –initiation of offset

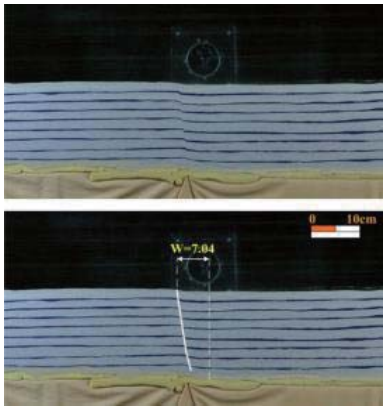

Step 2 –middle of test

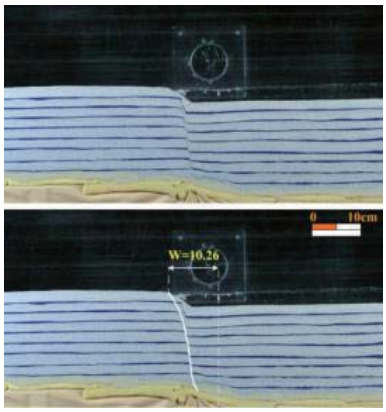

Step 3 –3 cm offset

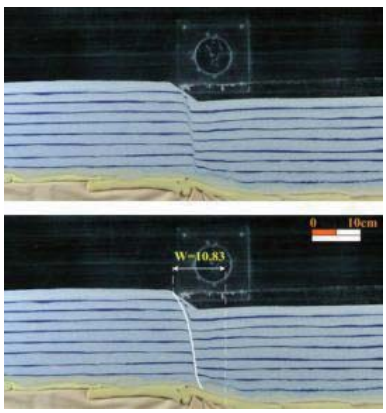

Step 4 –additional 0.7 cm offset

Fig. 7 Type 2 (offset twice under 24-hour duration) shear band propagation photos

the shear band first developed when there was a 3 cm offset after a waiting time of 24 hours. In the second 3 cm offset, the second shear band initiated from the first shear band and propagated to the sand surface at a total offset ratio of 4.2% ~ 4.8%; this is consistent with the results from the Type 1 test. A comparison of Figs. 6 and 7 showed a nearly identical displacement pattern of the sand layer at the same offset distance. Because of the 24 hour waiting time in the Type 2 test, the 24 hour duration (after the internal stress and particle movement reached a balanced condition) did not cause an apparent difference in the shear band propagation or in the width of the influenced zone at the sand layer surface. Because the tests were performed under a dry sand condition (*i.e.*, no pore water pressure), triggering the offset under a delayed duration might not affect the shear band propagation.

Type 3: A 5 cm fault tip offset and a 1 cm offset introduced after creating the growth fault

Because the growth fault was created using another layer of sand on top of the normal fault induced by a 5 cm offset, another 1 cm offset was introduced to the growth fault. The second shear band propagated along the end of the first shear band, reaching the sand surface with a smaller offset ratio of 1.5% to 1.8%. After applying a second offset event to the fault growth, the shear band only developed along the end of the first shear band, instead of initiating a new shear band from the fault tip. Compared to the required offset ratio of Type 1 and Type 2, the required offset ratio for the Type 3 test was approximately 1/3 of the required offset ratio of approximately 4.2 ~ 4.8% in the Type 1 test. Thus, with another offset event in the presence of the growth fault, the shear band developed to the ground surface with a smaller offset ratio along the original shear band, compared to the case when only normal faulting was created. Figure 8 shows the shear band propagation photos for Type 3 tests.

The Type 1, 2, and 3 test results (the results of repeat tests are included) are summarized in Fig. 9 according to the $\Delta H/H$ variations versus W/H (*i.e.*, the offset ratio versus the normalized influenced width). The required offset ratio for propagating the shear band to the sand surface is approximately 4.8% (Types 1 and 2) and 1.5% (Type 3), as shown in Fig. 9. The test results also showed that the increased offset ratio also increased the influenced width at the sand surface, but as the shear band propagated to the sand surface, the influenced width reached a nearly constant value, regardless of how the offset ratio increased. Table 1 also presents the Types 1 and 3 test results.

5. SUMMARY AND CONCLUSIONS

Based on the geotechnical and geological survey of the Shanchiao fault, the fault remains a highly active normal fault. The drilling and dating information proved that a depository layer 100 to 700 m in thickness exists on top of the normal fault and that the deposition thickness was accumulated after several ruptures and deposition events. In this study, a sandbox was employed to simulate shear band propagation of a regular normal fault (one time offset of 6 cm) and growth normal fault. To understand the effect of the delayed offset of a normal fault, one of the tests triggered an offset twice (each offset was 3 cm) within 24 hour. In the sand box simulation, we examined the offset ratio

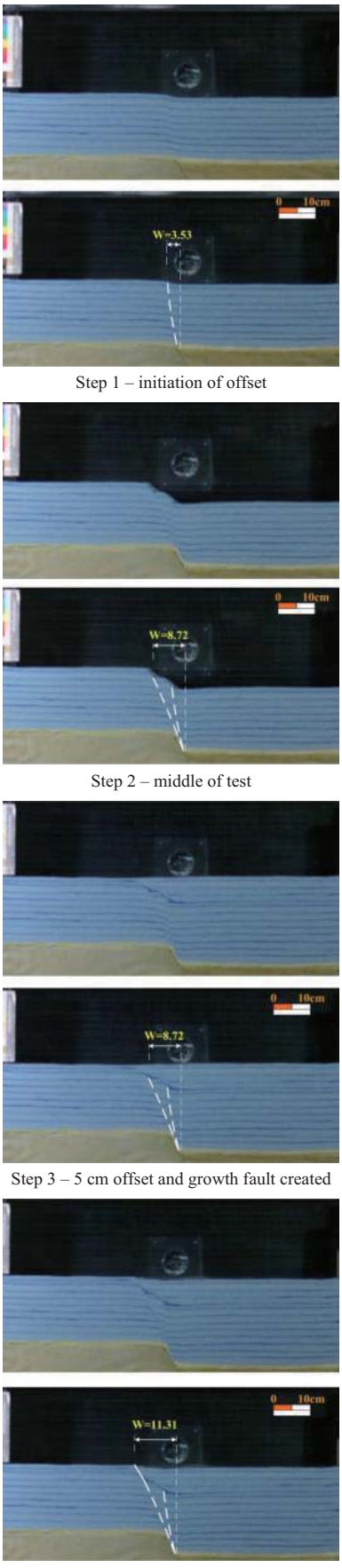

Fig. 8 Type 3 (growth normal fault) shear band propagation photos

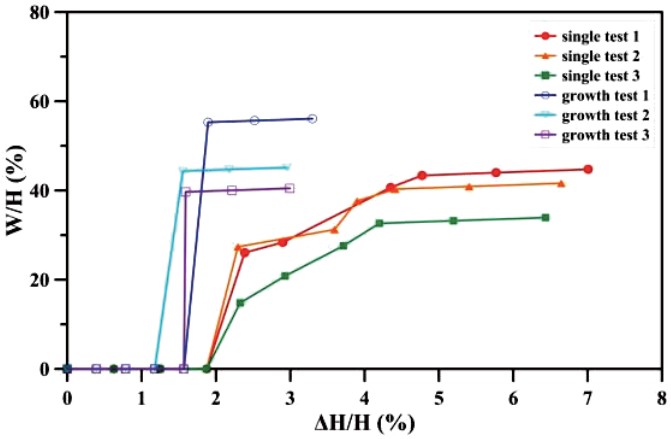

Fig. 9 Relationship of offset ratio ($\Delta H/H$) and normalized influenced width (W/H) for Type 1 (single) and Type 3 (growth) tests (each type of test was performed three times to avoid possible discrepancies of the results)

Table 1 Summary of shear band development for Type 1 (single layer) and 3 (with growth normal fault) tests

Type 1 and 3 sandbox test results		
Development of shear band	$\Delta H/H$	W/H
When first shear band is initiated (Type 1)	2.3% ~ 2.4%	15% ~ 27%
When first shear band develops to the sandy surface (Type 1)	4.2% ~ 4.8%	30% ~ 50%
1 cm of sand spread on the deformed normal fault layer		
The first shear band develops to the ground surface with growth normal fault (Type 3)	1.5% ~ 1.8%	40% ~ 55%

(defined as the offset displacement over the sand layer thickness) and the influenced width (normalized to the sand layer thickness) during the tests. Employing a thin layer of pigmented sand between regular sand layers achieved shear band development recognitions. Following displacement of the pigmented sand layer because of the induced offset in the fault tip, the shear band developed to the level of the displaced pigmented sand layer.

The increased offset ratio (*i.e.*, a normal fault was created) revealed a clear shear band gradually propagating upward. At the start of the test, the shear band initiated from the fault tip and gradually developed upward and toward the footwall side. After reaching a certain offset ratio value, the shear band propagated to the sand surface, revealing a clear tri-shear zone. For Type 1 and Type 2 tests, the required offset ratio for shear band propagation to the sand surface is approximately 4.8%. The waiting time for redistributing the stresses as performed in the Type 2 test did not show any test result difference compared to the Type 1 test. This might be because no water is present in the sandbox test. Without influence from pore water pressure, the stress can redistribute once the offset is terminated.

For the Type 3 test, another sand layer was spread onto the deformed normal fault and 1 cm of offset was introduced to the growth normal fault. The second shear band developed from the end of the first shear band and propagated to the sand surface with only a 1.5% offset ratio (approximately 0.3 cm). The tests performed in our study showed that, as the shear band propagated to the sand surface, the influenced width in all the tests remained unchanged, regardless of how the offset ratio increased.

The Type 3 test results (growth normal fault) also indicated that with a depositional layer on top of the deformed normal fault, the shear band in another offset event from the normal fault tip propagated to the ground surface with a much smaller offset ratio, but the influenced width at the ground surface was wider compared to the case without the growth normal fault. In addition, in the case of the growth normal fault with the occurrence of offset from the fault tip, the shear band continued from the end of the previous shear band and developed upward. The shear band developed to the ground surface with a much smaller offset ratio compared to a regular normal fault.

According to the sand box (under gravity condition) test results in this study, the differences between a regular normal fault and a growth normal fault can be easily differentiated. However, if the test results were to be applied and compared to the results from site investigation, the consideration of scale effects must be taken into account. Based on the site investigation and geological dating information of deposits in the Taipei basin, the Shanchiao fault, lying at the west rim of the Taipei basin, is a typical growth normal fault with a depositional thickness varying from 500 to 700 m. Although the fault tip might be deeply buried, based on our findings for sandy material, the shear band with a small offset ratio at the growth normal fault tip could develop to the ground surface. Hence for structures that are adjacent to a potential growth normal fault, the ground deformation characteristics need to be paid more attention to avoid any catastrophic failures of the structures.

REFERENCES

Bray, J. D. and Kelson, K. I. (2006). "Observations of surface fault rupture from the 1906 earthquake in the context of current practice." *Earthquake Spectra*, **22**, S69–S89.

Castelltort, S., Pochat, S., and Van den Driessche, J. (2004). "How reliable are growth strata in interpreting short-term (10 s to 100 s ka) growth structures kinematics?" *Comptes Rendus Geoscience*, **336**(2), 151–158.

Central Geological Survey, M. (2010). Active Fault Map of Taiwan (2010).

Chen, C. T., Lee, J. C., Chan, Y. C., and Lu, C. Y. (2010). "Growth normal faulting at the western edge of the metropolitan Taipei basin since the last glacial maximum, northern Taiwan." *Terrestrial Atmospheric and Oceanic Sciences*, **21**(3), 409–428.

Cheng, C. T., Lee, C. T., Lin, P. S., Lin, B. S., Tsai, Y. B., and Chiou, S. J. (2010). "Probabilistic Earthquake Hazard in Metropolitan Taipei and Its Surrounding Regions." *Terrestrial Atmospheric and Oceanic Sciences*, **21**(3), 429–446.

Egholm, D. L., Sandiford, M., Clausen, O. R., and Nielsen, S. B. (2007). "A new strategy for discrete element numerical models: 2. Sandbox applications." *Journal of Geophysical Research-Solid Earth*, **112**(B5), BO5204.

Ever Transit International Co. Limited (1999). The Shanchiao Fault investigation report of C. K. S. Airport to Taipei MRT system construction project (in Chinese).

Gawthorpe, R. and Hardy, S. (2002). "Extensional fault-propagation folding and base-level change as controls on growth-strata geometries." *Sedimentary Geology*, **146**(1-2), 47–56.

Gawthorpe, R. L., Sharp, I., Underhill, J. R., and Gupta, S. (1997). "Linked sequence stratigraphic and structural evolution of propagating normal faults." *Geology*, **25**(9), 795–798.

Huang, S. Y., Rubin, C. M., Chen, Y. G., and Liu, H. C. (2007). "Prehistoric earthquakes along the Shanchiao fault, Taipei Basin, northern Taiwan." *Journal of Asian Earth Sciences*, **31**(3), 265–276.

Hus, R., Acocella, V., Funiciello, R., and De Batist, M. (2005). "Sandbox models of relay ramp structure and evolution." *Journal of Structural Geology*, **27**(3), 459–473.

Kelson, K. I., Kang, K. H., Page, W. D., Lee, C. T., and Cluff, L. S. (2001). "Representative styles of deformation along the Chelungpu fault from the 1999 Chi-Chi (Taiwan) earthquake: Geomorphic characteristics and responses of man-made structures." *Bulletin of the Seismological Society of America*, **91**(5), 930–952.

Konagai, K. (2005). "Data archives of seismic fault-induced damage." *Soil Dynamics and Earthquake Engineering*, **25**(7-10), 559–570.

Lee, C. T. and Wang, Y. (1988). "Quaternary stress changes in northern Taiwan and their tectonic implication." *Proc. Geol. Soc. China*, 154–168.

Lee, W. J. and Hamada, M. (2005). "An experimental study on earthquake fault rupture propagation through a sandy soil deposit." *Journal of Structure Engineering/Earthquake Engineering*, JSCE, **22**, 1s–13s.

Lin, C. Z. (2005). "Shanchiao fault and geological structure of west edge of Taipei basin." *Symposium on Volcanic Activities and the Shanchiao Fault in the Taipei Metropolis*, 191–199 (in Chinese).

Liu, H. C., Su, T. W., Lee, J. F., Ji, T. J., and Lin, C. Z. (2000). *Activity of Shanchiao Fault and Effect on Safety of Engineering Work*. MOEA 2000 Research and Development Monograph (in Chinese).

Lu, C. Y., Angelier, J., Chu, H. T., and Lee, J. C. (1995). "Contractional, transcurrent, rotational and extensional tectonics - examples from northern Taiwan." *Tectonophysics*, **246**(1-3), 129–146.

Nicol, A., Walsh, J., Berryman, K., and Nodder, S. (2005). "Growth of a normal fault by the accumulation of slip over millions of years." *Journal of Structural Geology*, **27**(2), 327–342.

Nollet, S., Vennekate, G. J. K., Giese, S., Vrolijk, P., Urai, J. L., and Ziegler, M. (2012). "Localization patterns in sandbox-scale numerical experiments above a normal fault in basement." *Journal of Structural Geology*, **39**, 199–209.

Patton, T. L. (2005). "Sandbox models of downward-steepening normal faults." *Aapg Bulletin*, **89**(6), 781–797.

Pochat, S., Castelltort, S., Choblet, G., and Van Den Driessche, J. (2009). "High-resolution record of tectonic and sedimentary processes in growth strata." *Marine and Petroleum Geology*, **26**(8), 1350–1364.

Resources Engineering Services, Inc. (1999). "Road gallery range fault investigation report of Taipei MRT Xinzhuang line DK196 design case" (in Chinese).

Saltzer, S. D. (1992). "Boundary conditions in sandbox models of crustal extension — an analysis using distinct elements." *Tectonophysics*, **215**(3-4), 349–362.

Seyferth, M. and Henk, A. (2006). "A numerical sandbox: high-resolution distinct element models of halfgraben formation." *International Journal of Earth Sciences*, **95**(2), 189–203.

Taylor, S. K., Nicol, A., and Walsh, J. J. (2008). "Displacement loss on growth faults due to sediment compaction." *Journal of Structural Geology*, **30**(3), 394–405.

Teng, L. S. (1996). "Extensional collapse of the northern Taiwan mountain belt." *Geology*, **24**(10), 949–952.

Wang, J. H. (2008). "Urban seismology in the Taipei metropolitan area: review and prospective." *Terrestrial Atmospheric and Oceanic Sciences*, **19**(3), 213–233.

Yu, S. B., Kuo, L. C., Punongbayan, R. S., and Ramos, E. G. (1999). "GPS observation of crustal deformation in the Taiwan-Luzon region." *Geophysical Research Letters*, **26**(7), 923–926.